Journal of Colloid and Interface Science xxx (2017) xxx-xxx

Contents lists available at ScienceDirect

Journal of Colloid and Interface Science

journal homepage: www.elsevier.com

Regular Article

A spectroscopic sensing platform for MARCKS protein monolayers

Joaquín Klug[a], María Fernanda Torresan[b], Florencia Lurgo[b], Graciela Borioli[c,*], Gabriela I. Lacconi[b,*]

[a] CONICET and Facultad de Ciencias Exactas y Naturales, Universidad Nacional de Cuyo, Padre Jorge Contreras 1300, CP5500 Mendoza, Argentina
[b] INFIQC-CONICET, Dpto. de Fisicoquímica, Facultad de Ciencias Químicas, Universidad Nacional de Córdoba, Haya de La Torre-Medina Allende, Ciudad Universitaria, RA-5000 Córdoba, Argentina
[c] CIQUIBIC-CONICET, Dpto. de Química Biológica, Facultad de Ciencias Químicas, Universidad Nacional de Córdoba, Haya de La Torre-Medina Allende, Ciudad Universitaria, RA-5000 Córdoba, Argentina

ARTICLE INFO

Article history:
Received 22 May 2017
Received in revised form 23 August 2017
Accepted 24 August 2017
Available online xxx

Keywords:
Silver nanoparticles electrodeposition
SERS active platforms
Intrinsically unstructured proteins
MARCKS
Langmuir-Blodgett monolayers

ABSTRACT

We developed a highly sensitive silicon platform, suitable to assess the molecular organization of protein samples. Prototype platforms were obtained using different electrochemical protocols for the electrodeposition of Ag-nanoparticles onto the hydrogenated silicon surface. A platform with high Surface Enhanced Raman Scattering efficiency was selected based on the surface coverage and the number density of particles size distribution. The performance of the platform was determined by studying the interaction of Myristoylated Alanine-Rich C Kinase Substrate (MARCKS) protein with the substrate according to its molecular organization. The chemical and structural characteristics of MARCKS molecules were examined under two configurations: i) a disordered distribution given by a MARCKS solution drop deposited onto the platform and, ii) a compact monolayer transferred to the platform by the Langmuir-Blodgett method. Raman spectra show vibrational bands of Phenylalanine and Lysine residues specific for the protein effector domain, and evidence the presence of alpha helix structure in both configurations. Moreover, we distinguished the supramolecular order between the compact monolayer and random molecular distribution. The platforms containing Ag-nanoparticles are suitable for studies of protein structure and interactions, advancing a methodological strategy for our long term goal, which is to explore the interaction of proteins with model membranes.

1. Introduction

Raman spectroscopy is a particularly useful technique for chemical identification of biomolecules (proteins, lipids, polypeptides, etc.) in membrane model systems [1–4]. This analytical method is based on the inelastic scattering of monochromatic radiation resulting from interaction of the radiation with the sample, providing a molecular fingerprint of the material. It is an advantageous method for biophysical studies in real-time as it is non-invasive and can be applied in a wide variety of sample conditions such as different environment, aggregation state and amount of material. However, a significant limitation lies in the inherent weakness of the Raman scattering. Surface-enhanced Raman spectroscopy (SERS), coherent anti-Stokes Raman spectroscopy (CARS) and tip-enhanced Raman spectroscopy (TERS) are alternatives that overcome this drawback with remarkable enhancement of Raman scattering, showing adequate sensitivity and spatial resolution for the research of proteins and lipid membranes [5–7].

The enhancement of Raman signals of molecules adsorbed on "SERS active" metallic nanostructures (Ag or Au) is produced by the electromagnetic fields highly localized on the hot-spots, with the excitation of surface plasmons on the metal surface, either in solution or supported on a solid platform [8]. In SERS experiments using supported nanostructures, the molecules are adsorbed onto the solid substrate and, after being illuminated with visible radiation, the scattered light is collected from very small localized volumes through an optical microscope objective. Thus, the analysis of Raman spectra obtained by setting up a confocal system, provides detailed chemical and structural information with spatial resolution in the micrometer range. In particular, interactions that regulate biomembrane function can be explored using vibrational spectroscopy, with minimal perturbation [8].

The aim of this work is the optimization of SERS-active platforms for the study of intrinsically unstructured proteins (IUPs) [9]. We are particularly interested in using SERS in future studies to explore the interaction of IUPs with model membranes. IUPs are particularly interesting for several reasons: first, the fact that they are evolutionarily selected [10] indicates that they may perform their task more efficiently than structured proteins; second, their crucial role in global cellular processes such as signal transduction, cell cycle progression and transcription control, suggests that they may be involved in complex interactions with many partners or with supramolecular structures [11]; and third, they are elusive to standard methods of characterization [12]. Interactions are critical for the multiple functions of

* Corresponding authors.
Email addresses: gborioli@fcq.unc.edu.ar (G. Borioli); glacconi@mail.fcq.unc.edu.ar (G.I. Lacconi)

https://doi.org/10.1016/j.jcis.2017.08.081
0021-9797/

IUPs and, their interaction with membranes is certainly relevant to normal development [13–15]. The Myristoylated Alanine-Rich C Kinase Substrate (MARCKS) is an IUP with multiple functions based on its interactions with membranes [16–18], which is a fundamental condition implicated in various diseases such as neuroblastoma and respiratory tract related diseases [19–22]. MARCKS is a well-known link of signal transduction cascades involving PKC, and participates in brain development, phagocytosis, mitosis, cellular migration and adhesion, among other important processes. It is enriched in rafts where it cross-links actin filaments with plasma membrane and synaptic vesicles, by a complex calcium/calmodulin dependent process that is regulated by MARCKS phosphorylation and N-terminal myristoylation [23]. MARCKS association to membrane is mediated by a hydrophobic-electrostatic switch, located at the effector domain (ED) [24–27]. The interaction depends on ionic strength [28], and the content of acidic phospholipids and the curvature of membranes [29,30]. It triggers lateral segregation of phosphatidylinositol 4,5-bisphosphate (PIP_2) [31], thereby generating dynamic domains in the membrane that are related to cell signaling [32].

Our current approach focuses on the experimental analysis of the SERS signals of the pure protein. We have proceeded in a stepwise manner, as shown in the graphical abstract. Initially, we adjusted the conditions for Ag electrodeposition in order to obtain a distribution of Ag nanoparticles (AgNPs) fixed on the silicon platform with good properties as SERS substrate. The SERS performance was then assessed using a Rhodamine 6G (Rhod) probe, and finally, the selected Si-AgNPs platform was used as SERS support of a pure Langmuir-Blodgett (L-B) MARCKS monolayer. Detection of the main functional groups in the SERS active residues of the protein was achieved by comparing the intensity of vibrational modes of the silicon-supported monolayer with those on the AgNPs (SERS active sites) in the same sample. Spectroscopic analysis was complemented by Scanning Electron Microscopy (SEM) images and Energy-dispersive X-ray spectroscopy (EDS) in order to assess the topological compositional distribution of species on the platform.

Our results show evidence of direct interaction between the MARCKS effector domain (ED) and the AgNPs surface on the platform. Alpha helix structure and specific vibrational bands of Phenylanine (Phe) and Lysine (Lys) are observed when the protein ED interacts with the platform. Furthermore, Raman signals depend on the supramolecular order in the system, that is, a compact monolayer transferred to the platform by the Langmuir-Blodgett method, versus a random molecular distribution of a deposited drop. We conclude that the Si-AgNPs platforms are suitable for detailed studies of IUP proteins structure and interactions, thereby advancing a methodological strategy for our long term goal of exploring their interactions with model membranes.

2. Experimental section

2.1. Chemicals and materials

All aqueous solutions (electrolyte in the electrochemical cell and subphase for the monolayers) were prepared from analytical grade reagents and purified water (18.2 MΩ cm resistivity) using a Millipore Milli-Q system. The electrolyte for silver electrodeposition was $KClO_4$ (J.T. Baker) with $AgClO_4$ (BDH Chemicals Ltd.). The aqueous solutions for the subphase of MARCKS monolayers were prepared with 145 mM NaCl (MERCK). The MARCKS protein was purified by affinity chromatography using pETMARCKS, constructed by cloning the human MARCKS cDNA (996 bp) in the pET15-B vector (GenScript, USA Inc) [33]. Protein stocks were typically 1 μg/μl of protein in buffer of pH 7.4 containing 0.5 M NaCl, 20 mM Tris–HCl, 300 mM imidazole 300 and 8 M urea.

2.2. Cleaning and pretreatment of silicon surface

Hexagonal samples were cut from *n*-Si(1 1 1) wafers (1–20 Ω cm, Wafer World Inc.). Samples were first cleaned in an ultrasonic ethanol bath and the pretreatment of the silicon surface involved sequential oxidation and etching steps. A very thin oxide film was grown by immersion of silicon in a basic peroxide solution bath (30% H_2O_2: 28–30% NH_4OH: H_2O; 1:1:5 v/v) [34,35] during 10 min. at 80 °C, and after etching in a 50% HF/40% NH_4F (1:7) solution (3 min) a hydrogenated surface was obtained. After each step, samples were rinsed with Milli-Q water and dried with ultrapure N_2.

2.3. Ag nanoparticles electrodeposition and characterization

AgNPs were electrodeposited onto the hydrogenated silicon in an electrochemical home-made Teflon® cell. The *n*-Si(1 1 1)-H wafers were placed in the bottom of the cell exposing an 0.430 cm^2 area to the solution and the electrical contact was done at the backside of the wafer with In-Ga eutectic alloy. The counter electrode was a platinum ring, and a silver wire immersed in the Ag^+ electrolyte was the quasi-reference electrode. All potentials are quoted versus the Ag/Ag^+ (1 mM) quasi-reference electrode ($E_{Ag°/Ag+} = -0.30$ V versus the potential of saturated calomel electrode). The electrolyte used for silver deposition was 0.1 M $KClO_4$ + 1.0 mM $AgClO_4$ at pH 3.0 previously deoxygenated by pure nitrogen bubbling. Caution: manipulation of perchlorate salts is potentially hazardous. Different potential-time programs were applied to the electrode at 25 °C with a microcomputer controlled Autolab PGSTAT 30 (ECO CHEMIE) potentiostat/galvanostat. The morphology of AgNPs on the Si(1 1 1) platform was examined using a Field Emission Gun Scanning Electron Microscope (FE-SEM) Zeiss, ΣIGMA. Images were acquired with 8 kV of acceleration voltage. These platforms did not require metallic coating for SEM analysis. The SEM images were processed and analyzed with ImageJ software (Java) [36], and three regions (2 × 2 $μm^2$) selected at random for each SEM image (24 $μm^2$) were considered. The resulting particle mean number densities are shown in the histograms in Fig. 1.

2.4. Analysis of SERS activity with a probe molecule

The SERS activity of platforms was determined by using Rhodamine 6G (Rhod) as a probe molecule. A drop of 1.0×10^{-3} M aqueous Rhod solution was deposited onto the platforms, which were subsequently (after 10 min) rinsed and dried at ambient conditions. Raman and SERS spectra were obtained with a LABRAM-HR 800 Horiba Jobin Yvon microscope Raman system equipped with a He-Ne laser (632.8 nm). The laser power at the sample was set below 1.5 mW to minimize local laser-induced heating. The laser beam positioned through an Olympus microscope objective 100× lens (0.9 numerical aperture), irradiated 1.0 $μm^2$ area on the sample. The characteristic signal of silicon at 520.7 cm^{-1} was used for the spectrometer calibration. Raman spectra of Rhod and protein molecules under different configurations (drop or Langmuir-Blodgett monolayer transferred onto platforms), were recorded in a wavenumber range of 200–3500 cm^{-1}, with a spectral resolution of ~1.5 cm^{-1} for an exposure time of 10 s, for each measurement.

The Raman enhancement factor (F_{SERS}(Rhod)) for each platform was calculated with the ratio between integrated SERS intensities of the signal at 1648 cm^{-1} (I_{1648}), from adsorbed Rhod on the Si-AgNPs

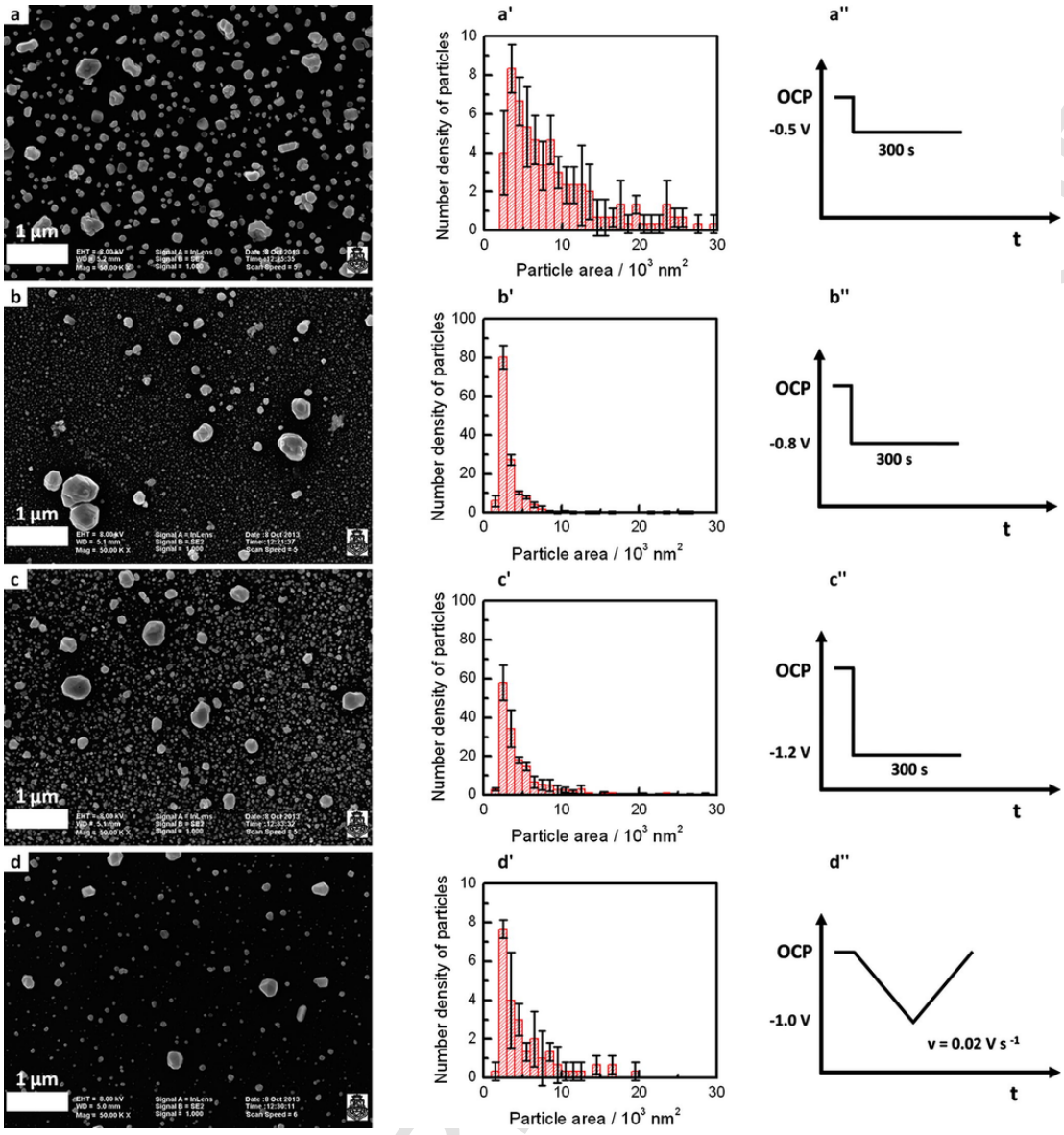

Fig. 1. SEM images (a–d) and histograms of AgNPs size distribution (a'–d') for silver electrodeposition on silicon platforms obtained by different potential-time programs (a''–d''). Error bars are the resulting number densities of particles from three regions (2×2 µm^2) selected at random for each SEM image (24 µm^2) and correspond to standard deviations. For further information see Table 1.

platform, and those corresponding to absence of AgNPs (I_{REF}). By considering all experimental parameters (concentration, time of spectrum recording, laser wavelength and power) as constant, F_{SERS}(Rhod) can be calculated using Eq. (1) [37].

$$F_{SERS}(\text{Rhod}) = I_{1648}/I_{REF} \quad (1)$$

2.5. MARCKS purification

Human recombinant MARCKS was purified by affinity chromatography using a plasmid constructed for that purpose. The complete DNA of the human gene was custom cloned (GeneScript USA Inc.) in the pET15b vector to construct the plasmid pMARCKS. The vector introduces a string of aminoacids (MGSSHHHHHHSSGLVPRGSH) which harbors the histidine tag that provides affinity for a specific resin column. The protein was purified from liquid cultures of *E. coli* containing pMARCKS using Novagene resin, and eluted in a 300 mM imidazole, 0.5 M NaCl, 20 mM Tris and 8 M urea buffer, pH 7.4. This protein preparation was characterized by SDS-PAGE, interfacial monolayers, Dynamic Light Scattering (DLS) and Spectroscopy. Electrophoresis and DLS results showed that MARCKS elutes with urea as a rather homogeneous population of particles with a hydrodynamic diameter of 26 nm (Fig. S1). Minor marginally represented populations of 270 and ~1000 nm were also observed by scattering. Purification without urea yields mainly aggregated protein. Quantification was done with the Bradford assay (Bio-Rad Bradford kit). Prior linearization of the standard curve with lisozyme as the standard protein was required. Calculated PI of human MARCKS without the his-tag is 4.39 and its calculated MW is 31664.77 Da.

2.6. Langmuir-Blodgett film and drop deposition

Monolayers were constructed by spreading small volumes of protein stock solutions onto the surface of pure MilliQ (R) water, or of NaCl at 145 mM and 50 mM. Aqueous stock 1 nmol/μL solutions of purified recombinant MARCKS protein (see previous section) were diluted in 150:200:30 Chloroform/Methanol/stock. About 100 μL of this dilution were slowly spread in a 273 cm^3 KSV NIMA (KSV, Finland) trough with a surface area of approximately 170 cm^3. After a 5 min wait for solvent evaporation, slow compression was performed by closing the barriers at a compression speed of 10 cm^2/min; the target pressure was 15 mN/m. After another 5 min stabilization wait, a single monolayer was transferred onto the platform submerged in the subphase prior to spreading, using the KSV NIMA LB dipper system, with the rate of withdrawal through the monolayer being 2 mm/min. Another configuration used to study the interaction between disordered MARCKS molecules and the Si-AgNPs platform involved the deposition of a drop (10 μL) of 1 nmol/μL MARCKS stock solution onto the SERS substrate. As a blank control, equivalent samples were deposited onto the silicon platform without AgNPs.

2.7. Characterization of MARCKS on the platforms

Raman and SERS spectra of protein supported on the platform were recorded with the micro-Raman spectrometer described in the *Analysis of SERS activity with a probe molecule.* Optical images and SERS spectra of samples containing MARCKS monolayers were acquired on freshly L-B transferred specimens or on a freshly deposited drop. After that, SEM and Energy Dispersive Spectrometry (EDS) analysis were carried out on the same platform. The corresponding spectra and images were then correlated, in order to obtain topographic and morphologic information of the different protein arrangements on the platform.

Different molecular arrangements could be easily identified through the optical images. In these experiments, the scattered intensities are presented in absolute values. Raman imaging of SERS signals was performed using the Raman imaging system incorporating a piezo-stage for the sample movement, exposing 12 × 12 μm^2 area to the focused He-Ne laser (spatial resolution of 1 μm and laser power of 0.5 mW). SERS spectra were acquired at every pixel of the image and the spectral mapping was achieved with colors assigned to Raman band intensities (signal area after baseline corrections).

The large depth of field characteristic of SEM microscopy enabled focusing of a large area of the sample; simultaneous qualitative information of the distribution of elements on the surface was obtained using an X-ray detector Energy Dispersive Spectrometer (EDS) and a Scanning Electron Microscope (FE-SEM) Zeiss, ΣIGMA.

3. Results and discussion

3.1. Electrodeposition of AgNPs on silicon platforms. Assessment of the SERS activity

The application of complex potential-time programs and the changing of electrolyte composition have been shown to be useful for controlling the size and distribution of deposited crystallites [38–40]. Thus, we used different electrochemical procedures for the deposition of silver nanoparticles (AgNPs) onto hydrogenated n-type silicon (1 1 1) oriented wafers, in order to obtain optimal conditions for SERS-active platforms.

Potential values for nucleation and growth of silver clusters were determined by analyzing the electrochemical behavior of the hydrogenated silicon electrodes (Si-H). Fig. S2 in the supplementary material shows the potentiodynamic profile of Si-H in 0.1 M $KClO_4$ + 1 mM $AgClO_4$ aqueous solution at pH 3.0, when a cyclic potential scan at 0.02 V s^{-1} has been applied. Two main current peaks (at around −0.46 V and −0.8 V) are observed in the cathodic potential scan, associated with the silver ion electroreduction on the semiconductor surface and on the silver crystallites, respectively. Upon reversing the potential sweep direction, deposition of silver continues until the potential reaches 0.0 V and no dissolution current is evidenced. Based on the potentiodynamic results, we assayed different potential-pulse programs to control the amount, distribution and size of electrodeposited AgNPs.

Application of various single potential pulses, or potential sweeps, to the Si-H electrodes resulted in different platforms. Fig. 1 shows the SEM images, the number density of particles size distribution (note that the histograms show distributions for particles smaller than 30.000 nm^2), and the respective potential-time programs. The percentage of silver covered area was determined as the fraction of the surface occupied by NPs on a representative ∼24 μm^2 area of the sample (Table 1).

The SEM images in Fig. 1 show that the entire surface is covered with particles of different sizes in all cases. Data in Table 1 show that when silver is deposited by a simple pulse at moderately negative potential (−0.5 V), the area covered is also moderate, and the number density of particles is very low (Fig. 1a). The presence of a few aggregates of particles on platform (a) is also evident. On the other hand, the histogram shows that the number density of deposited particles varies in a continuous way for sizes between 2000 and 30000 nm^2. There is a significant amount of Ag plasmonic particles with characteristic dimensions (with a diameter of around 140 nm for our experimental conditions), which have greater surface plasmon resonance effect and produce the major contribution to the enhancement.

When the pulse is at very negative potentials (−0.8 and −1.2 V), a high density of small particles is observed together with the presence of a few giant Ag crystallites (Fig. 1b and c). On the other hand, very low cathodic charge is consumed when silver is deposited by the potentiodynamic program d", with a low percentage of covered area and remarkable inhomogeneity of particles as revealed by SEM (Fig. 1d and Table 1).

Surface coverage and number of NPs are not the most important parameters for a SERS active substrate. The size and shape of the Ag-NPs formed, and the proximity between them, in terms of the resonance conditions of the surface plasmon, are very critical to increase Raman scattering. The efficiency of Raman enhancement on two different points of each platform, chosen at random, was determined by SERS spectra (average of 10 spectra with 10 s acquisition time) of

Table 1
Electrochemical charge of silver deposition (Q_{Ag}), percentage of silver covered area (% Area Ag) and SERS factor (F_{SERS}) for Si-AgNPs platforms given in Fig. 1.

Platform	Q_{Ag} / mC cm^{-2}	% Area (Ag)	F_{SERS} (Rhod) = I_{1648}/ I_{REF}
a	-12.45	19.4	$4.0x10^3$
b	-18.24	32.2	$3.6x10^3$
c	-26.81	31.3	$2.8x10^3$
d	-4.35	6.8	$1.4x10^3$

adsorbed Rhodamine 6G as a probe molecule. The most intense spectra for each platform are presented in Fig. 2. Mean values of approximate enhancement factor (F_{SERS}(Rhod)) from these measurements were calculated by the ratio of the 1648 cm^{-1} signal (C–C aromatic stretching vibration) intensities between the Si-AgNPs platform and the silicon surface [37]. Table 1 shows that mean F_{SERS} values are in the same order of magnitude. We have selected the potential pulse program "a" as the optimal and most simple procedure for a good SERS-active substrate, on the basis that it yields platforms with higher SERS intensity and less heterogeneous AgNPs.

3.2. Langmuir-Blodgett monolayers of MARCKS

In order to assess the quality of the AgNPs platforms for SERS studies of biological systems, we chose to focus on amphitropic IUPs because Raman has proved to be a powerful tool in differentiating among the multiple arrangements representing the signature of IUPs [41]. Thus, we used the MARCKS protein with two supramolecular arrangements, one organized as a Langmuir-Blodgett monoloayer and the other loosely deposited as a drop. MARCKS is a moderately acid protein with a putative charge of −32.3 at 7.4 which corresponds to the buffer pH. It is important to note that the Effector Domain (ED) of MARCKS, a tract of 26 aminoacids in the middle of the protein whose sequence is KKKKKRFSFKKSFKLSGFSFKKNKKE, represents 8% of the total length. Half of the residues in the ED are positive, mainly Lysines (that is, twelve of the total 27 lysines, the other 15 lysines being distributed along the rest of the sequence), and this high concentration of positive charge in the ED determines the – favorable – energetics of MARCKS domain formation with anionic and neutral phospholipids [42]. In addition, five of the six phenylalanines (F or Phe) present in MARCKS are located in the ED, allowing us to ascertain a molecular identification process involved in interactions with phospholipids, on the basis of changes observed in the Raman Phe signals. It is important to note that these aromatic residues penetrate in the hydrophobic core of acidic chains and, concomitantly, the positively charged Lysines (K or Lys) stay closer to the lipid phosphates [43]. Moreover, there are two other big hydrophobic residues in the MARCKS sequence, namely Leucines (L or Leu), one of which is within the ED, whilst the other lies in the N-terminal myristoylation domain together with the remaining Phe. This distinctive composition of the ED aided us in the interpretation of the SERS spectra.

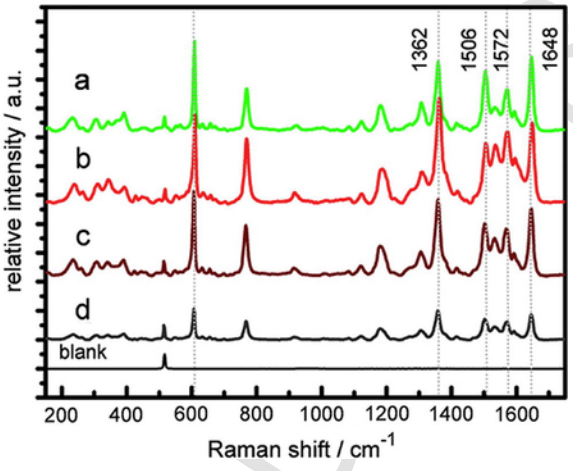

Fig. 2. SERS spectra of a dried drop of 1.0×10^{-3} M aqueous Rhodamine 6G solution adsorbed on the Si-AgNPs platforms obtained by silver electrodeposition. a–d refer to the different surfaces achieved by application of the potential-time programs presented in Fig. 1. In addition, a Raman spectrum of adsorbed Rhod on AgNPs-free silicon (blank) is included. All spectra were recorded at 633 nm excitation wavelength, the same laser power and integration time; besides, the spectra were normalized respect to the silicon signal at 520 cm^{-1}.

The Langmuir isotherm reveals that the interfacial behavior is representative of an expanded protein with high surface activity and remarkable hysteresis upon compression-decompression (Fig. S3). The adsorption behavior of MARCKS is typical of an IUP, with a critical subphase concentration of 300 nM and pseudo equilibrium surface lateral pressure of 19 mN/m, reached in less than 15 min [44,45]. These results denote that MARCKS is highly tensioactive and stable at the interface; therefore a protein monolayer may be spread and transferred onto the Si-AgNPs platform at 15 mN/m. The total transferred monolayer was about 2 cm^2, approximately corresponding to the area of both sides of the platform (not shown).

3.3. SERS detection of deposited MARCKS molecules

Fig. 3 shows a representative SEM image of the transferred L-B monolayer evidencing the presence of optically distinctive dense patches that probably arise due to water evaporation. These dense patches were also clearly observed in the Raman microscopy optical images. Their surface distribution is apparently independent of Ag particle location (Fig. S4). They contain a high concentration of protein and ions (as explained below based on EDS and SERS analysis), and remain intact long after sample preparation.

In order to obtain qualitative information about the composition of the transferred protein monolayer, EDS analysis was performed (Figs. 3 and S5). The elemental analysis shows correlations between the distribution of Na^+ and Cl^- ions on the platforms. Moreover, we find a higher density of these ions within the dense patches, suggesting that they may promote protein accumulation during water evaporation. This is consistent with no dense patches having been observed when the MARCKS monolayer was formed and transferred without NaCl in the subphase (results not shown).

It is important to note that the MARCKS monolayer is transferred throughout the entire platform surface, either accumulated in dense patches with higher salt concentration as discussed above, or dispersed outside these patches, as evidenced by SERS spectra discussed in the next section.

The selected SERS active platform "a" (Fig. 1) leads to a significant enhancement of the Raman scattering from protein monolayers. Fig. 4 shows the optical images and the representative SERS spectra of adsorbed MARCKS in two configurations: drop deposition (Fig. 4a) and L-B transference (Fig. 4b). We observe that signal intensification is obtained in both cases, yet significant enhancement is only evident in SERS spectra of the transferred monolayer (compare absolute intensities in Fig. 4a and b). Fig. 4 also includes a control experiment with the transferred protein monolayer onto a silicon area free of AgNPs (Fig. 4c). Details for the main signals in the spectra, and the respective assignments from literature sources, are summarized in Table 2 [46–52]. It is important to underline that the assignment of some Raman signals is based on individual amino acids [49–52], whereas in the present work the amino acids are not free but involved in bonds within the protein. As a consequence, frequencies in the SERS signals may have shifted with respect to those of the free amino acids.

In contrast to the monolayer configuration, when a drop of MARCKS solution is deposited and evaporated on the platform, no dense patches are observed (Fig. 4a). Based on the SERS spectra such as the one shown in Fig. 4a, we can identify particular amino acids that are directly adsorbed onto the particles. Signals at 1011, 1540 and 1585 cm^{-1} can be associated with Phe residues and those at 1175 and

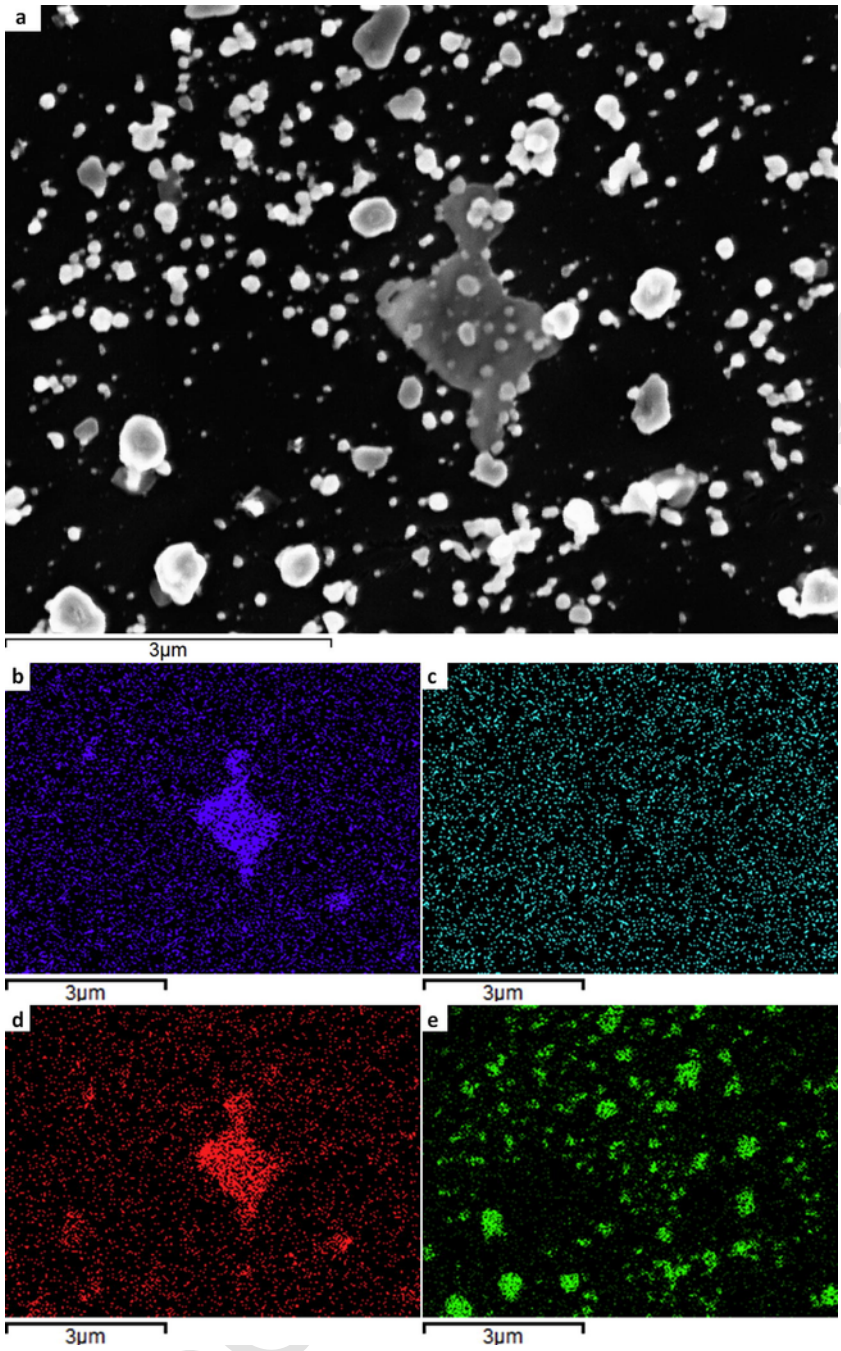

Fig. 3. SEM-EDS analysis of MARCKS monolayer transferred on Si-AgNPs platform: (a) SEM image of the sample and the corresponding X-ray maps for (b) Na (K_{a1}), (c) O (K_{a1}), (d) Cl (K_{a1}) and (e) Ag (L_{a1}) analysis.

1470 cm^{-1} with Lys residues present in the effector domain of MARCKS. Contrastingly, the intense signals at 3247 and 3349 cm^{-1} correspond to ν(N-H) stretching modes from NH_2 groups present in Asparagine, Glutamine and Arginine residues, which are located outside the ED. In addition, the presence of water in the system is revealed by the signal at 3431 cm^{-1}. We can conclude that the MARCKS molecules deposited as a drop are randomly arranged on the platform.

SERS spectra from the dense patches in the transferred monolayer (magenta ring in Fig. 4b) are much more intense (compare intensities scales in Fig. 4) and rather different from those recorded for the drop. Signals at 1230, 1563 and 1611 cm^{-1} correspond to vibrational modes of the aromatic ring of Phe and those at 1165, 1340 and 1450 cm^{-1} can be assigned to vibrational modes of the NH_3^+ group of Lys. In addition, a very intense signal at 3491 cm^{-1} indicates that water molecules are also present under this configuration. Finally, evidence of alpha helix structure arises from the Amide I band at 1650 and 1686 cm^{-1} from both SERS spectra [46]. It is interesting to note that SERS spectra recorded from spots focused outside the visualized protein dense patches show the same scattered signals, evidencing that the protein is present over the whole platform (Fig. S6).

We observe that the more conspicuous signals in the L-B configuration likely arise from Lys and Phe in the ED domain, suggesting

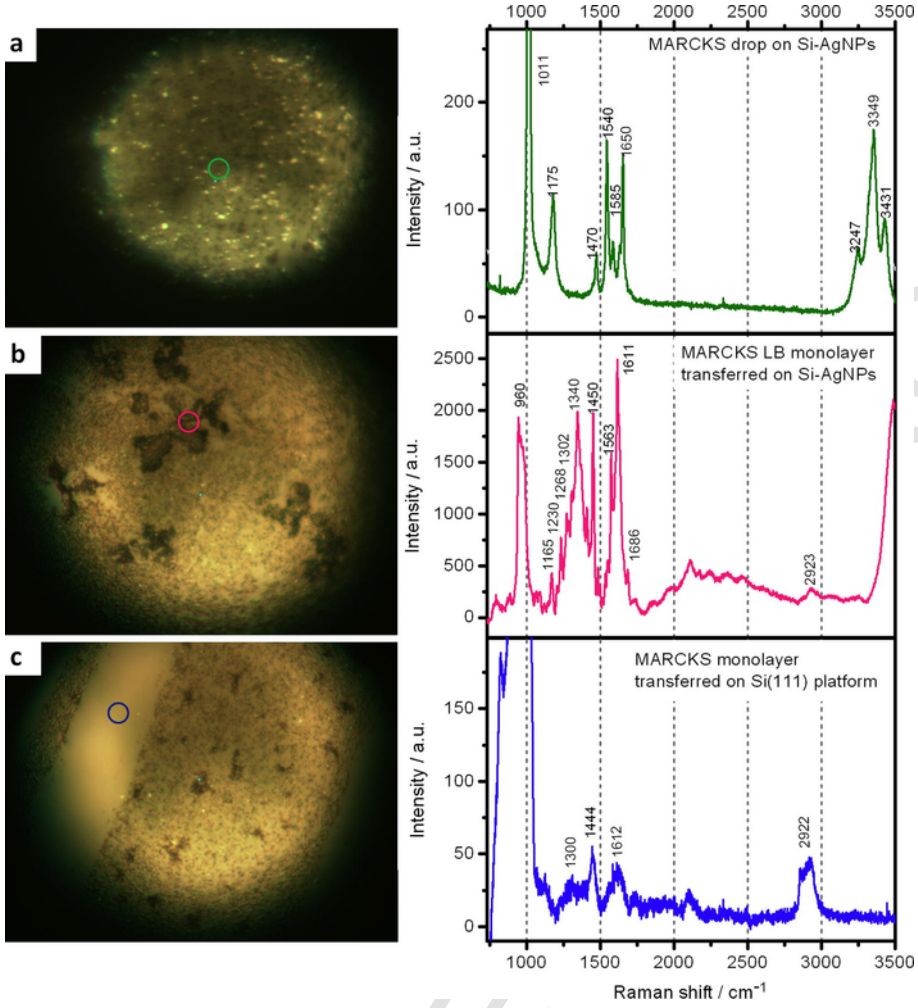

Fig. 4. Optical images and SERS or Raman spectra for MARCKS, (a) deposited as a drop on Si-AgNPs platforms (Si-AgNPs $MARCKS_{DROP}$); (b) monolayer transferred on Si-AgNPs platforms (Si-AgNPs $MARCKS_{LB}$) and (c) L-B transferred on the free-NPs area in the platform (Si-$MARCKS_{LB}$).

that the protein molecules maintain a certain order in the supramolecular arrangement when the whole monolayer is transferred.

In order to obtain complementary data, Raman imaging of Si-AgNPs platforms containing MARCKS transferred monolayer was carried out by using a piezo-electrical scanner with 1 μm step size. The scanned platform area was 12 × 12 μm^2 and SERS spectra were acquired at every pixel (144 pixels) of the image. Five spectra were collected with five seconds acquisition time at each pixel. MARCKS spectral mapping shown in Fig. 5 was achieved with different colors[1] assigned to Raman bands at 960 cm^{-1} (Two-phonon (2TO) process of Si(1 1 1)), 1340 cm^{-1} (Lys, CH bend) and 1611 cm^{-1} (Phe, ring CC str.). Intensity distribution (bands area after baseline corrections) on the platform was determined by correlating each spectrum with the optical image (Fig. 5a). In this manner, we could observe that the intensity distributions from Lys and Phe bands correspond to the same location in the platform, whereas the CH stretching shows a different pattern. In summary, main intensified signals can be readily assigned to Phenylalanine and Lysine residues belonging to the MARCKS ED directly adsorbed onto the SERS active substrate. As expected, we observe shifts in signal position and increased peak intensity in SERS with respect to Raman spectra of individual aminoacids, due to the fact that the residues in the protein are constrained by peptidic bonds. This result suggests a strong interaction between the ED aminoacid residues and the silver surface [49]. Finally, even though there is evidence of α-helix structure in the ED under both configurations (see Table 2), we have found changes in frequency and intensity that denote different supramolecular orders in the drop and the monolayer configurations: The CH-symmetric and antisymmetric vibrational modes at 2800–2900 cm^{-1} are absent in the spectra of the drop configuration, whereas the NH-vibrational modes at 3200–3500 cm^{-1} are present only in these spectra, denoting higher water content.

4. Conclusions

We have established a protocol for obtaining silicon platforms with silver electrodeposited nanoparticles, and assessed their suitability for SERS studies of biological specimens using an IUP protein. Moreover, the particle shape, size and distribution on the surface can be successfully controlled by the deposition potential. These platforms were used for comparative investigations of MARCKS under two configurations, deposited drop and L-B transference.

[1] For interpretation of color in 'Fig. 5', the reader is referred to the web version of this article.

Table 2
Tentative assignments of SERS bands for MARCKS deposited by a drop on the platform (Si-AgNPs-MARCKS$_{DROP}$), L-B transference on Si-AgNPs platforms (Si-AgNPs-MARCKS$_{LB}$) and Raman signals for MARCKS monolayer on Silicon platforms (Si-MARCKS$_{LB}$). Data correspond to the spectra in Fig. 4.

Tentative assignments	SERS Si-AgNPs-MARCKS$_{Drop}$ (cm^{-1})	SERS Si-AgNPs-MARCKS$_{LB}$ (cm^{-1})	Raman Si-MARCKS$_{LB}$ (cm^{-1})	Ref.
Two-phonon (2TO) process of Si(1 1 1)	–	~960	~960	[46]
Symm. ring CC str. **Phe**	1011	[a]	[a]	[47,48]
N-H wag **Lys**	1175	1165	–	[48]
Ring breath **Phe**	–	1230	–	[47,48]
CH_2 wag **Phe** and **Lys**	–	1302	1300	[47,48]
CH bend **Lys**	–	1340	–	[48]
CH_2 sciss. **Phe** and **Lys**	–	–	1444	[47,48]
CH_2 sciss.-NH def. **Lys**	1470	1450	–	[48]
Ring CC str. **Phe**	1540 1585	1563 1611	– 1612	[47,48]
Amida I – (α-helix)	1650	1686	–	[45,49]
CH str.	–--	2923	2922	[50]
ν(N-H) str. (NH_2) **Lys**	3244 3349		–	[50]
H_2O asymm. str.	3431	3491		[50]

[a] Signal superimposed with two-phonon (2TO) vibrational mode of silicon.

We can summarize the following points:

- Enhancement of Raman intensity is almost two orders of magnitude higher when the molecules are arranged in a monolayer transferred to the SERS active platform.
- SERS spectra of both configurations (compact monolayer versus random molecular distribution), show differences that emerge from the distinctive molecular order of these two arrangements. The drop configuration lacks the CH-signals indicating weak interactions between neighbor molecules, but has NH-vibrational modes suggesting higher water content.
- Similar spectral behavior is found in the CH vibrations region (2900–2930 cm^{-1}) for Raman spectra of MARCKS L-B recorded from two regions on the platform: the zones covered with Ag-nanoparticles and the Ag-free zones. This suggests that the ordered monolayer arrangement (with CH groups spatially distributed in a given orientation) is conserved after transferred to the platform, in the absence or presence of nanoparticles.
- An alpha helix structure may be observed only when MARCKS Effector Domain interacts with Ag-nanoparticles.
- The enhancement of the Phenylalanine and Lysine bands observed in the SERS spectra of MARCKS monolayer transferred onto the platform, suggests that Phenylalanine and Lysine, which are included in the Effector Domain, are interacting with the Ag-nanoparticles.
- The SERS active platforms proved to be an excellent solid support for the direct observation of biological material by SEM without the need to metalize the sample.

This work shows that the silicon platforms with silver nanoparticles, obtained by a defined electrodeposition protocol, could be valuable for exploring the interaction of proteins – especially intrinsically unstructured proteins – with model membranes. Raman spectroscopy

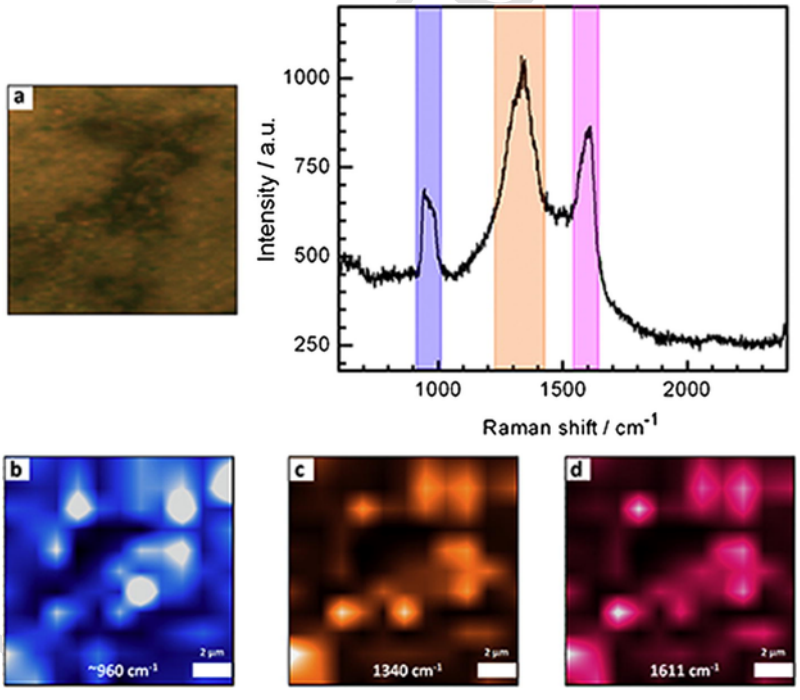

Fig. 5. Optical image (a), and SERS mapping from a 12 × 12 μm^2 area, for integration of signals at ~960 cm^{-1} (two-phonon, 2TO process of silicon) (b), 1340 cm^{-1} (Lys, CH bend) (c), and 1611 cm^{-1} (Phe, ring CC str.), for MARCKS monolayer transferred on the Si-AgNPs platform. The signals corresponding to each map are highlighted by blue (map b), orange (map c) and magenta (map d) bars in a representative spectrum taken at the dark protein aggregate seen in (a). Five spectra were collected with five seconds acquisition time at each pixel.

applied to sensors able to detect this kind of interactions would represent a great contribution to biomedical purposes.

Acknowledgements

This research has been supported with funds from INFIQC-CONICET, and CIQUIBIC-CONICET, FonCyT, SECyT-UNC. SEM-EDS characterization was provided by LAMARX-SNM of MINCyT. Raman microscopy facilities were provided by Laboratorio de Nanoscopía y Nanofotónica LANN-SNM of INFIQC (PME 1544). J. K. thanks CONICET for a Ph. D fellowship. We are also very grateful to Dr. L.A. Pérez for the Raman Imaging analysis and measurements, and for his great contribution to the discussion.

Conflicts of interest

The authors declare no actual or potential conflict of interest with other people or organizations.

Author contributions

All authors have approved the final version of the manuscript and contributed to the research and the article preparation as follows: JK, MFT, FL, GB and GL performed the experiments and discussed results; JK, GAB and GIL analyzed the data and prepared the manuscript. The authors declare that there are no competing financial interests.

Appendix A. Supplementary material

Supplementary data associated with this article can be found, in the online version, at http://dx.doi.org/10.1016/j.jcis.2017.08.081.

References

[1] T. Büchner, D. Drescher, H. Traub, P. Schrade, S. Bachmann, N. Jakubowski, J. Kneipp, Anal. Bioanal. Chem. 406 (2014) 7003.
[2] S. Dai, X. Zhang, Z. Du, Y. Huang, H. Dang, Colloid Surf. B: Biointerfaces 42 (2005) 21.
[3] T.G. Spiro, Biological Applications of Raman Spectroscopy: Raman Spectra and the Conformations of Biological Macromolecules, vol. 1, Wiley Interscience New York, 1987.
[4] L. Chen, X. Han, J. Yang, J. Zhou, W. Song, B. Zhao, W. Xu, Y. Ozaki, J. Colloid Interf. Sci. 360 (2011) 482.
[5] M.C. Giocondi, D. Yamamoto, E. Lesniewska, P. Milhiet, T. Ando, C. Le Grimellec, Biochim. Biophys. Acta 1798 (2010) 703.
[6] N.P. Ivleva, M. Wagner, A. Szkola, H. Horn, R. Niessner, C. Haisch, J. Phys. Chem. B 114 (2010) 10184.
[7] Z.D. Schultz, I.W. Levin, Annu. Rev. Anal. Chem. 4 (2011) 343.
[8] Ying Hui Ngo, Whui Lyn Then, Wei Shen, G. Garnier, J. Colloid Interface Sci. 409 (2013) 59.
[9] H.J. Dyson, P.E. Wright, Nat. Rev. Mol. Cell Biol. 6 (2005) 197.
[10] P. Tompa, BioEssays 25 (2003) 847.
[11] P.E. Wright, H.J. Dyson, Curr. Opin. Struct. Biol. 19 (2009) 31.
[12] J.D. Forman-Kay, T. Mittag, Structure 21 (2013) 1492.
[13] A.M. Cardozo Gizzi, B.L. Caputto, Crit. Rev. IUBMB Life 65 (2013) 584.
[14] Y. Perez, M. Maffei, I. Amata, M. Arbesú, M. Pons, Protoc. Exch. (2013) https://doi.org/10.1038/protex.2013.094.
[15] G.A. Borioli, Curr. Protein Pept. Sci. 12 (2011) 685.
[16] M.M. Myat, S. Anderson, L.H. Allen, A. Aderem, Curr. Biol. 7 (1997) 611.
[17] J.J. Ramsden, Int. J. Biochem. Cell Biol. 32 (2000) 475.
[18] S. Dulong, S. Goudenege, K. Vuillier-Devillers, S. Manenti, S. Poussard, P. Cottin, Biochem. J. 382 (2004) 1015.
[19] S.C. Morash, D. Byers, H. Cook, Biochim. Biophys. Acta 1487 (2000) 177.
[20] M. Singer, L.D. Martin, B.B. Vargaftig, J. Park, A.D. Gruber, Y. Li, K.B. Adler, Nat. Med. 10 (2004) 193.
[21] V.N. Uversky, C.J. Oldfield, A.K. Dunker, Annu. Rev. Biophys. 37 (2008) 215.
[22] V. Uversky, Expert Rev. Proteomics 7 (2010) 543.
[23] G. Vergeres, S. Manenti, T. Weber, C. Sturzinger, J. Biol. Chem. 270 (1995) 19879.
[24] H. Taniguchi, S. Manenti, J. Biol. Chem. 268 (1993) 9960.
[25] S. McLaughlin, A. Aderem, Trends Biochem. Sci. 20 (1995) 272.
[26] J.T. Seykora, M. Myat, L. Allen, J. Ravetch, A. Aderem, J. Biol. Chem. 271 (1996) 18797.
[27] A. Arbuzova, A. Schmitz, G. Vergeres, Biochem. J. 362 (2002) 1.
[28] J. Kim, T. Shishido, X. Jiang, A. Aderem, S. McLaughlin, J. Biol. Chem. 269 (1994) 28214.
[29] A. Gambhir, G. Hangya, M. Lyne, I. Zaitseva, D. Cafiso, J. Wang, D. Murray, S. Pentyala, S. Smith, S. McLaughlin, Biophys. J. 86 (2004) 2188.
[30] M. Bubb, R. Lenox, A. Edison, J. Biol. Chem. 274 (1999) 36472.
[31] M. Glaser, S. Wanaski, C.A. Buser, V. Boguslavsky, W. Rashidzada, A. Morris, M. Rebecchi, S.F. Scarlata, L.W. Runnels, G.D. Prestwich, J. Chen, A. Aderem, J. Ahni, S. McLaughlin, J. Biol. Chem. 271 (1996) 26187.
[32] S.L. Swierczynski, P. Blackshear, J. Biol. Chem. 270 (1995) 13436.
[33] M.C. Gaggiotti in phD Thesis, FCQ-UNC, Córdoba Argentina, 2011.
[34] J. Flidr, Y.C. Huang, M.A. Hines, J. Chem. Phys. 111 (1999) 6970.
[35] W. Kern, D. Puotinen, RCA Rev. 31 (1970) 187.
[36] C.A. Schneider, W.S. Rasband, K.W. Eliceiri, Nat. Methods 9 (2012) 671.
[37] S. Nie, S.R. Emory, Science 275 (1997) 1102.
[38] S.C. Kung, W. Xing, K.C. Donavan, F. Yang, R.M. Penner, Electrochim. Acta. 55 (2010) 8074.
[39] C.I. Vázquez, G.F. Andrade, M.L. Temperini, G.I. Lacconi, J. Phys. Chem. C 118 (2014) 4167.
[40] M.B. Quiroga Argañaraz, C.I. Vázquez, G.I. Lacconi, J. Electroanal. Chem. 639 (2010) 95.
[41] C.D. Syme, E.W. Blanch, C. Holt, J. Jakes, M. Goedert, L. Hecht, L.D. Barron, Eur. J. Biochem. 269 (2002) 148.
[42] G. Denisov, S. Wanaski, P. Luan, M. Glaser, S. McLaughlin, Biophys. J. 74 (1998) 731.
[43] W. Zhang, E. Crocker, S. McLaughlin, S. Smith, J. Biol. Chem. 278 (2003) 21459.
[44] M.C. Gaggiotti, M. Del Boca, G. Castro, B.L. Caputto, G.A. Borioli, Biopolymers 91 (2009) 710.
[45] M.F. Torresan, in Final Dissertation, FCQ-UNC Córdoba, Argentina, 2012.
[46] S. Olsztyńska-Janus, M. Gąsior-Głogowska, K. Szymborska-Małek, B. Czarnik-Matusewicz, M.A. Komorowska, in: Biomedical Engineering, Trends, Research and Technologies, vol. 91, Riejka, Croatia, 2011 (Chapter 4).
[47] F.M. Liu, B. Ren, J.W. Yan, B.W. Mao, Z.Q. Tian, J. Electrochem. Soc. 149 (2002) G95.
[48] E. Podstawka, Y. Ozaki, L.M. Proniewicz, Appl. Spectr. 59 (2005) 1516.
[49] S. Stewart, P.M. Fredericks, Spectrochim. Acta A 55 (1999) 1641.
[50] N.C. Maiti, M.M. Apetri, M.G. Zagorski, P.R. Carey, V.E. Anderson, J. Am. Chem. Soc. 126 (2004) 2399.
[51] S. Signorelli, S. Cannistraro, A.R. Bizzarri, Appl. Spectrosc. 71 (5) (2017) 823.
[52] A.L. Jenkins, R.A. Larsen, T.B. Williams, Spectrochim. Acta A 61 (2005) 1585.